Research Square

Preprints are preliminary reports that have not undergone peer review.
They should not be considered conclusive, used to inform clinical practice,
or referenced by the media as validated information.

Predictive value of a nomogram model based on ultrasound and clinical features for axillary lymph node metastasis in patients with breast cancer: a retrospective cohort study

Jinli Yu
Nantong Hospital of Traditional Chinese Medicine
Sunan Cao
Nantong Hospital of Traditional Chinese Medicine
Ming Li
Medical School of Nantong University
Xiaoyi Deng
Aoyang Hospital Affiliated to Jiangsu Universiy
Tao Zhang
19931067@qq.com

Nantong Third People's Hospital

Article

Keywords: Breast cancer, Axillary lymph node metastasis, Nomogram model, Ultrasound

Posted Date: November 18th, 2026

DOI: https://doi.org/10.21203/rs.3.rs-11364762/v1

License: This work is licensed under a Creative Commons Attribution 4.0 International License. Read Full License

Additional Declarations: No competing interests reported.

Abstract

Breast cancer (BC) is the most common malignancy in women, and axillary lymph node metastasis (ALNM) is closely associated with poorer prognosis and governs treatment decision-making. Current assessment relies mainly on sentinel lymph node biopsy, which is invasive and delays preoperative planning. This study aims to explore the predictive value of a nomogram model based on ultrasound and clinical features for ALNM in patients with breast cancer (BC). The clinical data of 193 BC patients treated in two hospitals from January 2022 to December 2024 were enrolled and retrospectively analyzed, of which, the clinical data of 113 patients from Nantong Hospital of Traditional Chinese Medicine were randomly divided into the training and internal validation cohorts at a 7:3 ratio, a predictive nomogram model for ALNM was constructed in the training cohort using a logistic regression to identify independent risk factors, and its performance was subsequently evaluated. Internal and external validations were carried out using the clinical data respectively from the internal validation cohort and the external validation cohort (80 patients) collected from Nantong Third People's Hospital. CA125, elasticity modulus ratio, unclear boundaries, irregular edges, and blood flow resistance index were identified as risk factors for ALNM. Receiver operating characteristic (ROC) curve analysis, calibration curve analysis, and decision curve analysis (DCA) demonstrated that the nomogram model established on these factors exhibited good discrimination, calibration, and clinical validity for predicting ALNM. Consistent results were also obtained in internal and external validation cohorts. The nomogram model based on ultrasound and clinical features demonstrates a promising predictive value for ALNM in BC patients, this study may provide a new auxiliary method for preoperative diagnosis of ALNM in BC patients. However, larger-scale multicenter validations are necessary to improve the generalizability of our model.

Background

Breast cancer (BC) is one of the most common malignant tumors among women worldwide, with an increasing incidence rate every year.[1] Its incidence rate is particularly high among women aged 40–60 years, particularly around the menopausal transition. BC is now the most frequently diagnosed cancer in women and the second leading cause of cancer death worldwide, with statistics indicating that more than 400,000 patients die from BC each year.[2] The pathogenesis of BC involves multiple factors, including genetic, lifestyle, endocrine, and environmental factors.[3, 4] BC occurs when there are abnormal expressions or mutations in cell cycle regulatory genes, which further leads to dysregulation of the cell cycle, promotes the uncontrolled proliferation of cancer cells and impairs apoptosis, ultimately resulting in tumor formation. The pathological subtypes of BC primarily include invasive ductal carcinoma (IDC), invasive lobular carcinoma (ILC), mucinous carcinoma, papillary carcinoma, and triple-negative BC (TNBC). IDC is the most common histological subtype of BC, accounting for approximately 70–80% of BC cases.[5]

Axillary lymph node metastasis (ALNM) is a common manifestation of BC and identified as an adverse prognostic indicator. The BC patients with ALNM are often classified as having locally advanced or progressive disease, which is associated with a relatively poorer prognosis.[6, 7] In current clinical practice, sentinel lymph node biopsy (SLNB) is accepted as the standard procedure for early detection of ALNM. However, it is an invasive procedure, and intraoperative assessment of the sentinel lymph node deprives patients of the opportunity to participate in treatment planning. Therefore, developing non-invasive diagnostic techniques for accurately identifying preoperative ALNM has been of vital importance. With the rapid development of high-frequency ultrasound and color Doppler ultrasound technology, ultrasound has become one of the primary imaging diagnostic methods for breast lesions. It can more clearly display the morphology, boundaries, internal echoes, calcifications, and blood flow of breast and lymph node lesions. In recent years, accumulating evidence indicates that certain ultrasound imaging features of

BC, including tumor size, quadrant location, local invasion, pathological and molecular subtypes, shape, growth pattern, boundaries, posterior acoustic features, calcifications and echoes, are associated with ALNM and may aid in predicting axillary lymph node status.[8–12]. This study aimed to explore the preoperative prediction value of a nomogram model based on ultrasound and clinical features for ALNM in BC patients.

Methods

Patients

A total of 193 BC patients treated in two hospital from January 2022 to December 2024 were enrolled into this study, including 113 patients from Nantong Hospital of Traditional Chinese Medicine and 80 patients from Nantong Third People's Hospital.The patients aged 25–88 years, with a mean age of 59.73 ± 14.91 years old. A retrospective analysis was conducted on the baseline clinical and pathological data, and ultrasound imaging features of all enrolled patients. Inclusion criteria were as follows: (1) female patients; (2) those with histopathologically confirmed invasive ductal carcinoma (IDC); (3) those with a definite pathological diagnosis of axillary lymph nodes; (4) those with a single breast lesion; (5) those with complete clinical baseline data; (6) those with complete and clear ultrasound imaging features. Exclusion criteria were as follows: (1) patients with a history of other malignant tumors; (2) those with other concurrent breast diseases; (3) those with a history of breast augmentation;(4) those with distant metastasis; (5) those receiving anticancer treatment before surgery. The clinical data of all study subjects are presented in Table 1.

Table 1
Comparison of patient data between two hospitals

Variables	Total cases (n = 193)	Cases from Nantong Hospital of Traditional Chinese Medicine (n = 113)	Cases from Nantong Third People's Hospital (n = 80)	Statistics	*P*
Age, Mean ± SD	59.73 ± 14.91	59.45 ± 15.09	60.12 ± 14.73	t=-0.31	0.758
Number of pregnancies, M (Q_1, Q_3)	1.00 (1.00, 3.00)	2.00 (1.00, 3.00)	1.00 (1.00, 2.25)	Z=-0.66	0.506
Number of vaginal deliveries, M (Q_1, Q_3)	1.00 (1.00, 1.00)	1.00 (1.00, 1.00)	1.00 (1.00, 1.00)	Z=-0.34	0.734
Maximum diameter, M (Q_1, Q_3)	2.50 (1.80, 3.50)	2.50 (1.70, 3.50)	2.50 (1.80, 3.52)	Z=-0.23	0.817
CEA(ng/mL), M (Q_1, Q_3)	1.46 (0.82, 1.84)	1.40 (0.81, 1.84)	1.48 (0.89, 1.86)	Z=-0.49	0.625
CA153(U/mL), M (Q_1, Q_3)	13.00 (7.30, 19.00)	13.00 (6.90, 19.00)	12.85 (7.39, 18.62)	Z=-0.03	0.974
CA125(U/mL), M (Q_1, Q_3)	13.20 (8.83, 17.60)	13.30 (8.88, 17.81)	12.70 (8.82, 17.02)	Z=-0.39	0.694
E_{mean}, M (Q_1, Q_3)	290.75 (225.11, 361.07)	290.75 (222.08, 357.79)	303.39 (228.72, 379.60)	Z=-0.71	0.477
E_{max}, M (Q_1, Q_3)	850.49 (650.99, 1098.08)	850.49 (631.20, 1080.95)	859.73 (667.62, 1122.86)	Z=-0.45	0.652
E_{min}, M (Q_1, Q_3)	87.77 (54.44, 109.35)	87.77 (54.44, 108.77)	87.33 (54.37, 110.64)	Z=-0.15	0.880
E_{sd}, M (Q_1, Q_3)	150.82 (90.47, 182.39)	149.67 (90.05, 182.39)	150.94 (92.38, 181.59)	Z=-0.15	0.878
Elasticity modulus ratio, M (Q_1, Q_3)	3.56 (2.31, 5.73)	3.65 (2.33, 5.80)	3.54 (2.31, 5.68)	Z=-0.21	0.834
Number of miscarriages, M (Q_1, Q_3)	0.00 (0.00, 1.00)	0.00 (0.00, 1.00)	0.00 (0.00, 1.00)	Z=-0.82	0.414
Blood flow resistance index, M (Q_1, Q_3)	0.60 (0.50, 0.70)	0.60 (0.50, 0.70)	0.60 (0.50, 0.70)	Z=-0.16	0.873
Elasticity score, M (Q_1, Q_3)	4.00 (3.00, 4.00)	4.00 (3.00, 4.00)	4.00 (3.00, 4.00)	Z=-0.45	0.650
Gestational hypertension, n(%)				χ^2=0.60	0.439

Abbreviation: ALNM, Axillary lymph node metastasis; CA125, Cancer antigen 125; CA153, Cancer antigen 153; CEA, Carcinoembryonic antigen.

Variables	Total cases (n = 193)	Cases from Nantong Hospital of Traditional Chinese Medicine (n = 113)	Cases from Nantong Third People's Hospital (n = 80)	Statistics	*P*
No	175 (90.67)	104 (92.04)	71 (88.75)		
Yes	18 (9.33)	9 (7.96)	9 (11.25)		
Gestational diabetes, n(%)				χ^2=0.20	0.651
No	179 (92.75)	104 (92.04)	75 (93.75)		
Yes	14 (7.25)	9 (7.96)	5 (6.25)		
History of breastfeeding, n(%)				χ^2=0.00	0.986
No	128 (66.32)	75 (66.37)	53 (66.25)		
Yes	65 (33.68)	38 (33.63)	27 (33.75)		
Location of the primary lesion, n(%)				-	0.792
Nipple	6 (3.11)	4 (3.54)	2 (2.50)		
Upper outer quadrant	112 (58.03)	67 (59.29)	45 (56.25)		
Lower outer quadrant	75 (38.86)	42 (37.17)	33 (41.25)		
Aspect ratio (greater than 1), n(%)				χ^2=0.22	0.641
No	24 (12.44)	13 (11.50)	11 (13.75)		
Yes	169 (87.56)	100 (88.50)	69 (86.25)		
Uneven internal echo, n(%)				χ^2=0.16	0.685
No	22 (11.40)	12 (10.62)	10 (12.50)		
Yes	171 (88.60)	101 (89.38)	70 (87.50)		
Unclear boundary, n(%)				χ^2=0.03	0.870
No	47 (24.35)	28 (24.78)	19 (23.75)		
Yes	146 (75.65)	85 (75.22)	61 (76.25)		
Irregular edge, n(%)				χ^2=0.73	0.394
No	54 (27.98)	29 (25.66)	25 (31.25)		
Yes	139 (72.02)	84 (74.34)	55 (68.75)		
Irregular shape, n(%)				χ^2=0.16	0.689

Abbreviation: ALNM, Axillary lymph node metastasis; CA125, Cancer antigen 125; CA153, Cancer antigen 153; CEA, Carcinoembryonic antigen.

Variables	Total cases (n = 193)	Cases from Nantong Hospital of Traditional Chinese Medicine (n = 113)	Cases from Nantong Third People's Hospital (n = 80)	Statistics	*P*
No	29 (15.03)	16 (14.16)	13 (16.25)		
Yes	164 (84.97)	97 (85.84)	67 (83.75)		
Calcification, n(%)				χ^2=0.24	0.886
Coarse	17 (8.81)	9 (7.96)	8 (10.00)		
None	120 (62.18)	71 (62.83)	49 (61.25)		
Mild	56 (29.02)	33 (29.20)	23 (28.75)		
Blood flow grading, n(%)				χ^2=0.44	0.933
0	23 (11.92)	13 (11.50)	10 (12.50)		
1	67 (34.72)	40 (35.40)	27 (33.75)		
2	61 (31.61)	37 (32.74)	24 (30.00)		
3	42 (21.76)	23 (20.35)	19 (23.75)		
ALNM, n(%)				χ^2=0.17	0.679
No	110 (56.99)	63 (55.75)	47 (58.75)		
Yes	83 (43.01)	50 (44.25)	33 (41.25)		

Abbreviation: ALNM, Axillary lymph node metastasis; CA125, Cancer antigen 125; CA153, Cancer antigen 153; CEA, Carcinoembryonic antigen.

Baseline clinical data of BC patients

The baseline clinical data of BC patients included the following indicators: age, number of pregnancies, number of miscarriages, number of vaginal deliveries, gestational hypertension, gestational diabetes, history of breastfeeding, ALNM, carcinoembryonic antigen (CEA) (ng/mL),cancer antigen (CA) 153 (U/mL), CA125 (U/mL).

Ultrasound imaging features of BC patients

Conventional ultrasound imaging features included the following indicators: location of the primary lesion, maximum diameter, aspect ratio greater than 1, homogeneous internal echoes, clarity of boundaries, regularity of edges, regularity of shape, calcification (none/mild/coarse), blood flow grading of the tumors assessed by Adler semi-quantitative analysis. [13] blood flow resistance index, shear wave elastography (SWE): maximum (E_{max}),mean (E_{mean}), and minimum (E_{min}) values of Young's modulus, and standard deviation (E_{sd}), elasticity score, and elasticity modulus ratio.

Statistical processing

In this study, 113 BC patients were randomly divided into a training cohort (79 cases) and a validation cohort (34 cases) at a ratio of 7:3. In addition, BC patients were categorized into non-metastatic and metastatic groups according to the presence or absence of ALNM. For continuous variables, those with a normal distribution, as assessed by the Kolmogorov-Smirnov D test, were expressed as mean ± SD, and comparisons between groups were made using independent t-tests; those without a normal distribution were expressed as median (interquartile range), and comparisons between groups were made using the Mann-Whitney U rank-sum test. Categorical data were expressed as composition ratios, and comparisons between groups were performed using the chi-square test or Fisher's exact test. The indicators that differed significantly between the non-metastatic and metastatic groups in the training cohort were included in an unconditional binary logistic regression model for univariate and multivariate analyses to identify risk factors for ALNM. The identified risk factors were then incorporated into a the binary logistic regression model to construct a nomogram prediction model based on ultrasound and clinical features. This model was evaluated using ROC curve analysis, Hosmer-Lemeshow goodness-of-fit test, calibration curves, and decision curve analysis (DCA). The clinical validity of this model for predicting ALNM was validated in both the internal and external validation cohorts. A p-value of less than 0.05 was considered statistically significant. All data processing and analyses were performed using R version 4.4.0, along with Zstats 1.0 platform (www.zstats.net).

Results

Comparison of patient data between two hospitals

The comparison of patient data between two hospitals revealed no significant differences ($P > 0.05$). The results are shown in Table 1.

Comparison of patient data between the training and internal validation cohorts

The comparison of patient data between the training set and internal validation cohorts revealed no significant differences ($P > 0.05$). The results are shown in Table 2.

Table 2
Comparison of data between training and internal validation cohorts

Variables	Cases from Nantong Hospital of Traditional Chinese Medicine (n = 113)	Internal validation cohort (n = 34)	Train cohort (n = 79)	Statistics	*P*
Age, Mean ± SD	59.45 ± 15.09	62.15 ± 12.82	58.29 ± 15.90	t = 1.25	0.214
Number of pregnancies, M (Q_1, Q_3)	2.00 (1.00, 3.00)	2.00 (1.00, 3.00)	1.00 (1.00, 2.50)	Z=-1.16	0.245
Number of vaginal deliveries, M (Q_1, Q_3)	1.00 (1.00, 1.00)	1.00 (1.00, 1.00)	1.00 (1.00, 1.00)	Z=-0.40	0.690
Maximum diameter, M (Q_1, Q_3)	2.50 (1.70, 3.50)	2.45 (1.70, 3.50)	2.50 (1.80, 3.55)	Z=-0.50	0.616
CEA (ng/mL), M (Q_1, Q_3)	1.40 (0.81, 1.84)	1.16 (0.80, 1.66)	1.51 (0.89, 1.88)	Z=-1.33	0.182
CA153 (U/mL), M (Q_1, Q_3)	13.00 (6.90, 19.00)	14.05 (6.90, 20.18)	13.00 (7.38, 18.75)	Z=-0.19	0.851
CA125 (U/mL), M (Q_1, Q_3)	13.30 (8.88, 17.81)	13.70 (9.82, 18.35)	13.00 (8.82, 17.05)	Z=-0.75	0.451
E_{mean}, M (Q_1, Q_3)	290.75 (222.08, 357.79)	270.40 (213.08, 315.35)	304.73 (229.67, 379.77)	Z=-1.84	0.065
E_{max}, M (Q_1, Q_3)	850.49 (631.20, 1080.95)	824.68 (559.93, 1022.27)	850.49 (667.41, 1120.88)	Z=-0.85	0.395
E_{min}, M (Q_1, Q_3)	87.77 (54.44, 108.77)	87.67 (53.70, 105.54)	87.77 (54.55, 111.12)	Z=-0.03	0.973
E_{sd}, M (Q_1, Q_3)	149.67 (90.05, 182.39)	124.72 (88.47, 182.26)	151.07 (92.27, 181.86)	Z=-0.45	0.652
Elasticity modulus ratio, M (Q_1, Q_3)	3.65 (2.33, 5.80)	3.84 (2.19, 7.37)	3.56 (2.41, 5.70)	Z=-0.24	0.807
Number of miscarriages, M (Q_1, Q_3)	0.00 (0.00, 1.00)	0.00 (0.00, 1.00)	0.00 (0.00, 1.00)	Z=-1.77	0.077
Blood flow resistance index, M (Q_1, Q_3)	0.60 (0.50, 0.70)	0.60 (0.50, 0.70)	0.60 (0.50, 0.70)	Z=-0.64	0.522
Elasticity score, M (Q_1, Q_3)	4.00 (3.00, 4.00)	3.00 (3.00, 4.00)	4.00 (3.00, 4.00)	Z=-0.89	0.373
Gestational hypertension, n(%)				χ^2=0.84	0.360
no	104 (92.04)	33 (97.06)	71 (89.87)		

Abbreviations: ALNM, Axillary lymph node metastasis; CA125, Cancer antigen 125; CA153, Cancer antigen 153; CEA; Carcinoembryonic antigen.

Variables	Cases from Nantong Hospital of Traditional Chinese Medicine (n = 113)	Internal validation cohort (n = 34)	Train cohort (n = 79)	Statistics	*P*
yes	9 (7.96)	1 (2.94)	8 (10.13)		
Gestational diabetes, n(%)				χ^2=1.84	0.175
No	104 (92.04)	29 (85.29)	75 (94.94)		
Yes	9 (7.96)	5 (14.71)	4 (5.06)		
History of breastfeeding, n(%)				χ^2=0.04	0.851
No	75 (66.37)	23 (67.65)	52 (65.82)		
Yes	38 (33.63)	11 (32.35)	27 (34.18)		
Location of the primary lesion, n(%)				-	0.614
Nipple	4 (3.54)	2 (5.88)	2 (2.53)		
Upper outer quadrant	67 (59.29)	21 (61.76)	46 (58.23)		
Lower outer quadrant	42 (37.17)	11 (32.35)	31 (39.24)		
Aspect ratio (greater than 1), n(%)				χ^2=0.14	0.705
No	13 (11.50)	5 (14.71)	8 (10.13)		
Yes	100 (88.50)	29 (85.29)	71 (89.87)		
Uneven internal echo, n(%)				χ^2=0.01	0.941
No	12 (10.62)	3 (8.82)	9 (11.39)		
Yes	101 (89.38)	31 (91.18)	70 (88.61)		
Unclear boundary, n(%)				χ^2=0.07	0.785
No	28 (24.78)	9 (26.47)	19 (24.05)		
Yes	85 (75.22)	25 (73.53)	60 (75.95)		
Irregular edge, n(%)				χ^2=3.06	0.080
No	29 (25.66)	5 (14.71)	24 (30.38)		
Yes	84 (74.34)	29 (85.29)	55 (69.62)		
Irregular shape, n(%)				χ^2=0.03	0.853
No	16 (14.16)	4 (11.76)	12 (15.19)		

Abbreviations: ALNM, Axillary lymph node metastasis; CA125, Cancer antigen 125; CA153, Cancer antigen 153; CEA; Carcinoembryonic antigen.

Variables	Cases from Nantong Hospital of Traditional Chinese Medicine (n = 113)	Internal validation cohort (n = 34)	Train cohort (n = 79)	Statistics	*P*
Yes	97 (85.84)	30 (88.24)	67 (84.81)		
Calcification, n(%)				χ^2=1.72	0.423
Coarse	9 (7.96)	1 (2.94)	8 (10.13)		
None	71 (62.83)	23 (67.65)	48 (60.76)		
mild	33 (29.20)	10 (29.41)	23 (29.11)		
Blood flow grading, n(%)				χ^2=2.32	0.508
0	13 (11.50)	4 (11.76)	9 (11.39)		
1	40 (35.40)	13 (38.24)	27 (34.18)		
2	37 (32.74)	13 (38.24)	24 (30.38)		
3	23 (20.35)	4 (11.76)	19 (24.05)		
ALNM, n(%)				χ^2=0.16	0.693
No	63 (55.75)	18 (52.94)	45 (56.96)		
Yes	50 (44.25)	16 (47.06)	34 (43.04)		

Abbreviations: ALNM, Axillary lymph node metastasis; CA125, Cancer antigen 125; CA153, Cancer antigen 153; CEA; Carcinoembryonic antigen.

Comparison of patient data between the metastatic and non-metastatic groups in the training cohort

Compared with the non-metastatic group, the indicators such as CA125 and CA153, and elasticity modulus ratio were significantly increased in the metastatic group, and the blood flow resistance index was significantly decreased in the metastatic group ($P < 0.05$). The lesions exhibited a higher proportion of unclear **boundaries and irregular edges** ($P < 0.05$). The results are shown in Table 3.

Table 3
Comparison of data between the metastatic and non-metastatic group in the training cohort

Variables	Cases of training cohort (n = 79)	Non-metastatic group (n = 45)	Metastatic group (n = 34)	Statistics	*P*
Age, Mean ± SD	58.29 ± 15.90	60.64 ± 15.72	55.18 ± 15.82	t = 1.53	0.131
Number of pregnancies, M (Q_1, Q_3)	1.00 (1.00, 2.50)	1.00 (1.00, 2.00)	2.00 (1.00, 2.75)	Z=-0.93	0.353
Number of vaginal deliveries, M (Q_1, Q_3)	1.00 (1.00, 1.00)	1.00 (1.00, 2.00)	1.00 (1.00, 1.00)	Z=-0.38	0.702
Maximum diameter, M (Q_1, Q_3)	2.50 (1.80, 3.55)	2.20 (1.60, 3.30)	2.65 (2.23, 3.60)	Z=-1.89	0.058
CEA (ng/mL), M (Q_1, Q_3)	1.51 (0.89, 1.88)	1.34 (0.78, 1.81)	1.60 (1.21, 2.31)	Z=-1.82	0.068
CA153 (U/mL), M (Q_1, Q_3)	13.00 (7.38, 18.75)	9.90 (6.61, 16.50)	15.80 (10.38, 20.50)	Z=-2.04	0.041
CA125 (U/mL), M (Q_1, Q_3)	13.00 (8.82, 17.05)	11.30 (7.40, 15.90)	15.05 (11.05, 20.17)	Z=-2.28	0.023
E_{mean}, M (Q_1, Q_3)	304.73 (229.67, 379.77)	304.73 (225.26, 381.14)	308.50 (239.36, 360.25)	Z=-0.25	0.801
E_{max}, M (Q_1, Q_3)	850.49 (667.41, 1120.88)	850.49 (629.56, 1125.33)	929.28 (697.54, 1095.21)	Z=-0.20	0.839
E_{min}, M (Q_1, Q_3)	87.77 (54.55, 111.12)	87.77 (61.27, 103.78)	80.12 (54.24, 114.27)	Z=-0.14	0.887
E_{sd}, M (Q_1, Q_3)	151.07 (92.27, 181.86)	151.07 (92.04, 184.32)	152.25 (94.60, 172.00)	Z=-0.14	0.887
Elasticity modulus ratio, M (Q_1, Q_3)	3.56 (2.41, 5.70)	2.69 (2.13, 3.53)	5.53 (4.40, 6.98)	Z=-5.30	< .001
Number of miscarriages, M (Q_1, Q_3)	0.00 (0.00, 1.00)	0.00 (0.00, 1.00)	0.00 (0.00, 1.00)	Z=-0.88	0.377
Blood flow resistance index, M (Q_1, Q_3)	0.60 (0.50, 0.70)	0.60 (0.50, 0.70)	0.50 (0.50, 0.60)	Z=-2.75	0.006
Elasticity score, M (Q_1, Q_3)	4.00 (3.00, 4.00)	4.00 (3.00, 4.00)	4.00 (3.00, 4.00)	Z=-0.56	0.579
Gestational hypertension, n(%)				χ^2=0.00	1.000
No	71 (89.87)	40 (88.89)	31 (91.18)		
Yes	8 (10.13)	5 (11.11)	3 (8.82)		
Gestational diabetes, n(%)				χ^2=0.00	1.000
No	75 (94.94)	43 (95.56)	32 (94.12)		
Yes	4 (5.06)	2 (4.44)	2 (5.88)		

Abbreviations:: ALNM, Axillary lymph node metastasis; CA125, Cancer antigen 125; CA153, Cancer antigen 153; CEA, Carcinoembryonic antigen.

Variables	Cases of training cohort (n = 79)	Non-metastatic group (n = 45)	Metastatic group (n = 34)	Statistics	*P*
history of breastfeeding, n(%)				χ^2=0.03	0.856
No	52 (65.82)	30 (66.67)	22 (64.71)		
Yes	27 (34.18)	15 (33.33)	12 (35.29)		
Location of the primary lesion, n (%)				-	0.909
Nipple	2 (2.53)	1 (2.22)	1 (2.94)		
Upper outer quadrant	46 (58.23)	27 (60.00)	19 (55.88)		
Lower outer quadrant	31 (39.24)	17 (37.78)	14 (41.18)		
Aspect ratio (greater than 1), n(%)				χ^2=0.00	1.000
No	8 (10.13)	5 (11.11)	3 (8.82)		
Yes	71 (89.87)	40 (88.89)	31 (91.18)		
Uneven internal echo, n(%)				χ^2=0.00	1.000
No	9 (11.39)	5 (11.11)	4 (11.76)		
Yes	70 (88.61)	40 (88.89)	30 (88.24)		
Unclear boundary, n(%)				χ^2=4.93	0.026
No	19 (24.05)	15 (33.33)	4 (11.76)		
Yes	60 (75.95)	30 (66.67)	30 (88.24)		
Irregular edge, n(%)				χ^2=13.11	< .001
No	24 (30.38)	21 (46.67)	3 (8.82)		
Yes	55 (69.62)	24 (53.33)	31 (91.18)		
Irregular shape, n(%)				χ^2=0.28	0.597
No	12 (15.19)	6 (13.33)	6 (17.65)		
Yes	67 (84.81)	39 (86.67)	28 (82.35)		
Calcification, n(%)				-	0.318
Coarse	8 (10.13)	5 (11.11)	3 (8.82)		
None	48 (60.76)	30 (66.67)	18 (52.94)		
Mild	23 (29.11)	10 (22.22)	13 (38.24)		
Blood flow grading, n(%)				χ^2=7.78	0.051

Abbreviations:: ALNM, Axillary lymph node metastasis; CA125, Cancer antigen 125; CA153, Cancer antigen 153; CEA, Carcinoembryonic antigen.

Variables	Cases of training cohort (n = 79)	Non-metastatic group (n = 45)	Metastatic group (n = 34)	Statistics	*P*
0	9 (11.39)	8 (17.78)	1 (2.94)		
1	27 (34.18)	18 (40.00)	9 (26.47)		
2	24 (30.38)	10 (22.22)	14 (41.18)		
3	19 (24.05)	9 (20.00)	10 (29.41)		

Abbreviations:: ALNM, Axillary lymph node metastasis; CA125, Cancer antigen 125; CA153, Cancer antigen 153; CEA, Carcinoembryonic antigen.

Analysis of risk factors for ALNM in BC patients

CA125 and CA153, elasticity modulus ratio,blood flow resistance index, and the proportions of unclear boundaries and irregular edges were separately incorporated into a binary logistic regression model. The analysis results showed that CA125, elasticity modulus ratio, blood flow resistance index, and unclear boundaries and irregular edges were risk factors associated with ALNM ($P < 0.05$). These indicators were entered into the binary logistic regression model simultaneously, and the analysis results revealed that the elasticity modulus ratio and irregular edges were independent high-risk factors for ALNM ($P < 0.05$). The results are shown in Table 4.

Table 4
Univariate and multivariate analyses of risk factors for ALNM in BC patients

Variables	Univariate analysis					Multivariate analysis				
	β	S.E	Z	*P*	OR (95%CI)	β	S.E	Z	*P*	OR (95%CI)
CA153 (U/mL)	0.01	0.01	0.56	0.575	1.01 (0.99 ~ 1.03)	-0.01	0.02	-0.48	0.630	0.99 (0.96 ~ 1.02)
CA125 (U/mL)	0.08	0.04	2.18	0.029	1.09 (1.01 ~ 1.17)	0.06	0.05	1.22	0.221	1.06 (0.96 ~ 1.18)
Elasticity modulus ratio	0.68	0.16	4.19	< .001	1.97 (1.44 ~ 2.71)	0.61	0.18	3.43	< .001	1.84 (1.30 ~ 2.60)
Unclear boundary										
No					1.00 (Reference)					1.00 (Reference)
Yes	1.32	0.62	2.13	0.033	3.75 (1.11 ~ 12.62)	1.06	0.87	1.22	0.223	2.88 (0.53 ~ 15.76)
Irregular edge										
No					1.00 (Reference)					1.00 (Reference)
Yes	2.20	0.67	3.26	0.001	9.04 (2.41 ~ 33.91)	1.83	0.84	2.17	0.030	6.24 (1.19 ~ 32.68)
Blood flow resistance index	-6.16	2.30	-2.69	0.007	0.00 (0.00 ~ 0.19)	-5.51	3.28	-1.68	0.093	0.00 (0.00 ~ 2.49)

Abbreviations: ALNM, Axillary lymph node metastasis; CA125, Cancer antigen 125; CA153, Cancer antigen 153; OR, Odds ratio, CI, Confidence interval.

Construction and evaluation of a nomogram prediction model in training cohort

The risk factors for ALNM, such as CA125, elasticity modulus ratio, blood flow resistance index, and unclear boundaries and irregular edges, were used to construct a nomogram prediction model using a logistic regression model, and the equation was as follows: Logit (P) = 0.06×CA125 + 0.61 × elasticity modulus ratio + 1.06 × unclear boundaries + 1.83×irregular edges − 5.51×blood flow resistance index − 2.81. The constructed prediction model was visualized using a nomogram (Fig. 1A).

The results of ROC curve analysis showed that the area under curve (AUC) of the nomogram prediction model was 0.90 (95%CI: 0.83–0.97) (Fig. 1B), and the accuracy, sensitivity, and specificity of this model were 0.84 (95%CI: 0.74–0.91), 0.89 (95%CI: 0.80–0.98), and 0.76 (95%CI: 0.62–0.91) respectively (Table 5). The calibration curve showed good consistency between the predicted curve and the ideal curve in this nomogram prediction model. Hosmer-Lemeshow goodness-of-fit test yielded $\chi^2 = 8.589$ ($P = 0.378$) (Fig. 1C). The DCA results showed that the

nomogram model could provide a net benefit in BC patients over a threshold probability range of 0.05–0.99 for ALNM prediction (Fig. 1D).

Table 5
Results of ROC curve analyses in three cohorts

Data	AUC (95%CI)	Accuracy (95%CI)	Sensitivity (95%CI)	Specificity (95%CI)	PPV (95%CI)	NPV (95%CI)	Cut off value
Training cohort	0.90 (0.83–0.97)	0.84 (0.74–0.91)	0.89 (0.80–0.98)	0.76 (0.62–0.91)	0.83 (0.73–0.94)	0.84 (0.71–0.97)	0.546
Internal validation cohort	0.84 (0.71–0.97)	0.76 (0.59–0.89)	0.89 (0.74–1.00)	0.62 (0.39–0.86)	0.73 (0.54–0.91)	0.83 (0.62–1.00)	0.546
External validation cohort	0.89 (0.82–0.96)	0.84 (0.74–0.91)	0.96 (0.90–1.00)	0.67 (0.51–0.83)	0.80 (0.70–0.91)	0.92 (0.81–1.00)	0.546

Abbreviations: AUC, Area under curve; ROC,Receiver operating characteristic; PPV, Positive predictive value; NPV, Negative predictive value.

Validation of the clinical applicability of nomogram prediction model

In the internal validation cohort, the results of the ROC curve analysis showed that the AUC of this nomogram prediction model was 0.84 (95%CI: 0.71–0.97) (Fig. 2A), and its accuracy, sensitivity and specificity were 0.76 (95%CI: 0.59–0.89), 0.89 (95%CI: 0.74–1.00), and 0.62 (95%CI: 0.39–0.86) respectively (Table 5). The calibration curve showed good consistency between the predicted curve and the ideal curve in this nomogram prediction model, Hosmer-Lemeshow goodness-of-fit test result yielded $\chi^2 = 10.414$ ($P = 0.237$). (Fig. 2B). The DCA results showed that the nomogram model could provide a net benefit in BC patients over a threshold probability range of 0.05–0.99 for ALNM prediction (Fig. 2C).

In the external validation cohort, the results of the ROC curve analysis showed that the AUC of this nomogram prediction model was 0.89 (95%CI: 0.82–0.96) (Fig. 3A), and its accuracy, sensitivity, and specificity were 0.84 (95%CI: 0.74–0.91), 0.96 (95%CI: 0.90–1.00), and 0.67 (95%CI: 0.51–0.83) respectively (Table 5). The calibration curve showed good consistency between the predicted curve and the ideal curve in the nomogram prediction model, the Hosmer-Lemeshow goodness-of-fit test result yielded $\chi^2 = 7.829$ ($P = 0.622$) (Fig. 3B). The DCA results showed that the nomogram model could provide a net benefit in BC patients over a threshold probability range of 0.05–0.99 for ALNM prediction(Fig. 3C).

Discussion

In the staging of BC, ALNM is a critical determinant of prognosis and treatment decision-making. Even when ALNM is present, appropriate treatment can still improve clinical prognosis. Management of ALNM therefore typically requires a comprehensive, multimodal approach that combines local control and systemic therapy. Local control is achieved through surgical resection of the primary tumor and affected lymph nodes, including procedures such as breast resection and axillary lymph node dissection. Systemic therapy, including chemotherapy, endocrine therapy, and targeted therapy, aims to control potential distant metastases and improve prognosis. Consequently, it is crucial to develop non-invasive diagnostic methods for the precise identification of preoperative ALNM. The results of this

study showed the nomogram model constructed based on ultrasound and clinical features demonstrated a promising predictive value for ALNM, and may provide a new auxiliary method for the preoperative diagnosis of ALNM in BC patients.

Currently, few studies have investigated the nomogram prediction models for ALNM in BC patients, and no nomogram prediction model has been widely applied in clinical practice. Furthermore, most studies have incorporated postoperative pathological features into their predictive models, which diminishes the clinical utility of preoperative prediction. However, the nomogram predictive models can offer the following several advantages;[14] (1) Intuitive: the nomogram can present information visually, and facilitate comprehension and clinical application by both physicians and patients; (2) accurate: the nomogram models are derived from extensive datasets and statistical calculations, thus yielding relatively accurate predictive results; (3) personalized: the nomogram models can be tailored to individual patient characteristics, incorporating multiple risk-related factors to offer personalized prediction, and lymph node metastasis in BC patients may be influenced by multiple factors.[15, 16] To construct such a nomogram model, it is crucial to identify the risk factors closely related to ALNM in BC patients. Therefore, in this study, we first compared the differential indicators between the metastatic and non-metastatic groups in the training cohort, and then incorporated these differential indicators into a binary logistic regression model, and the analysis results showed that CA125, the elasticity modulus ratio, unclear boundaries, irregular edges, and the blood flow resistance index were risk factors for ALNM, and the elasticity modulus ratio and irregular edges were independent high-risk factors for ALNM. CA125 is a biomarker primarily associated with ovarian cancer,[17], yet its effects in BC and ALNM remain under investigation. Some studies suggest that elevated CA125s may be linked to more advanced disease stages or poorer prognosis in BC patients.[18] However, the specific relationship between CA125 and ALNM is not fully established and may vary across individuals; further research is needed to clarify the significance of CA125 as a predictive marker in this context.The ultrasound examination shows that the unclear boundaries and irregular edges of the BC lesion are associated with greater tumor invasiveness. These features are widely regarded as signs of increased tumor aggressiveness and may indicate extension into surrounding tissues, thereby increasing the risk of lymph node metastasis.[19] Some studies[20] also suggest that the blood flow resistance index may be associated with tumor aggressiveness and the risk of lymph node metastasis. A lower blood flow resistance index indicates typically abundant angiogenesis and robust blood supply in tumors, which is often observed to be correlated with larger tumor size and higher clinical stage. SWE is an advanced ultrasound imaging technique used to assess tissue stiffness and elasticity. It provides quantitative information by measuring the propagation speed of shear waves within the tissue and is commonly used in tumor diagnosis and evaluation.[21–24] Among the important parameters derived from this examination is the elasticity modulus ratio, which reflects the stiffness contrast between tumor and surrounding tissue. An increased elasticity modulus ratio is often associated with malignant tumors, as malignant tumors are usually stiffer than benign ones.[25].

Based on the risk factors identified as being associated with ALNM, we developed a prediction model using multivariable logistic regression and visualized it as a nomogram. The clinical effectiveness of this model was evaluated using ROC curve, calibration curve, and DCA. The results indicated that this model had acceptable discrimination and consistency, demonstrating good clinical applicability. To further validate its clinical applicability, we performed both internal and external validation, and the results from both validation cohorts were generally consistent with those from the training cohort.

Limitations

Several limitations should be acknowledged in the present study. First, because of its retrospective design, inherent selection bias may have been introduced, and no formal sample-size calculation was performed. Second, the sample sizes of both the internal and external validation cohorts in this study were relatively small, which to some extent limited the breadth and depth of model validation; accordingly, in future research we plan to further expand the sample size and conduct multicenter studies to more comprehensively verify the accuracy and reliability of this model. Third, although multiple ultrasound and clinical features were incorporated, other factors that may exert an important influence on the occurrence of ALNM were not considered and should be explored and incorporated in subsequent studies. Finally, because only patients with invasive ductal carcinoma were enrolled and the participants came from two hospitals in a single region, the generalizability of the model to other pathological subtypes and populations requires further investigation; the nomogram should therefore serve only as an auxiliary preoperative tool and cannot replace sentinel lymph node biopsy in clinical decision-making.

Conclusion

The nomogram model constructed based on ultrasound and clinical features in this study demonstrates a promising predictive value for ALNM in BC patients. This study may provide a new auxiliary method for the preoperative diagnosis of ALNM and may assist clinicians in stratifying the risk of ALNM before surgery. However, it should be regarded as an auxiliary reference tool rather than a basis for directly optimizing treatment selection, and further multicenter prospective validations are warranted to confirm these findings.

Declarations

Ethical approval

This study was conducted in accordance with the ethical principles outlined in the Declaration of Helsinki and approved by Medical Ethics Committee of Nantong Hospital of Traditional Chinese Medicine (Tongzhongyuan [2022] Zi 002–37). Due to the retrospective nature of this study, the requirement for written informed consent was formally waived by the Medical Ethics Committee of Nantong Hospital of Traditional Chinese Medicine. All enrolled patients were adult females aged 25–88 years (mean age 59.73 ± 14.91 years). No vulnerable populations (such as pregnant women or cognitively impaired individuals) were involved in this study.

Competing interests

The authors declare that they have no competing interests.

Funding

This study was supported by Guiding Project of Nantong Science and Technology Plan (MSZ2022029)

Author Contribution

Jinli Yu: Data curation, Project administration, Writing–original draft, Sunan Cao: Data curation, Formal Analysis,Methodology, Writing–original draft. Ming Li and Xiaoyi Deng: Data curation, Software,Visualization, Writing–original draft. Tao Zhang: Conceptualization, Project administration, Writing–review and editing.

Data Availability

The datasets generated and/or analyzed during the current study are not publicly available due to patient privacy, but are available from the corresponding author on reasonable request

References

1. Bhardwaj, P. V. et al. Breast cancer in India: screening, detection, and management. *Hematol Oncol. Clin. North Am.* **38**, 123–135. 10.1016/j.hoc.2023.05.014 (2024).
2. Sung, H. et al. Global Cancer Statistics 2020: GLOBOCAN estimates of incidence and mortality worldwide for 36 cancers in 185 countries. *CA Cancer J. Clin.* **71**, 209–249. 10.3322/caac.21660 (2021).
3. Michaels, E. et al. Breast Cancer: Risk assessment, screening, and primary prevention. *Med. Clin. North. Am.* **107**, 271–284. 10.1016/j.mcna.2022.10.007 (2023).
4. Nolan, E. et al. Deciphering breast cancer: from biology to the clinic. *Cell* **186**, 1708–1728. 10.1016/j.cell.2023.01.040 (2023).
5. Neagu, A. N. et al. Proteomics-based identification of dysregulated proteins and biomarker discovery in invasive ductal carcinoma, the most common breast cancer subtype. *Proteomes* **11** 10.3390/proteomes11020013 (2023).
6. Zhang, L. L. et al. Correlation between extranodal invasion in axillary lymph node metastasis and prognosis of breast cancer patients. *Zhonghua Bing Li Xue Za Zhi*. **46**, 525–529. 10.3760/cma.j.issn.0529-5807.2017.08.002 (2017).
7. Qian, F. et al. Establishment of a logistic regression model nomogram for clinicopathological characteristics and risk factors with axillary lymph node metastasis in T1 locally advanced breast cancer: a retrospective study. *Gland Surg.* **13**, 871–884. 10.21037/gs-24-34 (2024).
8. Bai, X. et al. Ultrasound and clinicopathological characteristics of breast cancer for predicting axillary lymph node metastasis. *Clin. Hemorheol Microcirc*. **85**, 147–162. 10.3233/CH-231777 (2023).
9. Xiong, J. et al. Ultrasonography and clinicopathological features of breast cancer in predicting axillary lymph node metastases. *BMC Cancer*. **22**, 1155. 10.1186/s12885-022-10240-z (2022).
10. Zheng, B. et al. Novel model based on ultrasound predict axillary lymph node metastasis in breast cancer. *BMC Med. Imaging*. **23**, 135. 10.1186/s12880-023-01090-7 (2023).
11. Guo, Q. et al. Ultrasound features of breast cancer for predicting axillary lymph node metastasis. *J. Ultrasound Med.* **37**, 1345–1353. 10.1002/jum.14469 (2018).
12. Liu, X. et al. Diagnostic value of contrast-enhanced ultrasound for sentinel lymph node metastasis in breast cancer: an updated meta-analysis. *Breast Cancer Res. Treat.* **202**, 221–231. 10.1007/s10549-023-07063-2 (2023).
13. Adler, D. D. et al. Doppler ultrasound color flow imaging in the study of breast cancer: preliminary findings. *Ultrasound Med. Biol.* **16**, 553–559 (1990).
14. Balachandran, V. P. et al. Nomograms in oncology: more than meets the eye. *Lancet Oncol.* **16**, e173–180. 10.1016/S1470-2045(14)71116-7 (2015).
15. Wang, W. Y. et al. [Analysis of risk factors of axillary lymph node metastasis and prognosis in T1 breast cancer: a large-scale retrospective study based on the SEER database]. *Zhonghua Yi Xue Za Zhi*. **101**, 2152–2158. 10.3760/cma.j.cn112137-20201218-03392 (2021).

16. Lee, S. E. et al. Optimal treatment strategy for hormone receptor-positive human epidermal growth factor receptor 2-negative breast cancer patients with 1–2 suspicious axillary lymph node metastases on breast magnetic resonance imaging: upfront surgery vs. neoadjuvant chemotherapy. *Front. Oncol.* **13**, 936148. 10.3389/fonc.2023.936148 (2023).
17. Ren, A. H. et al. Mucin 13 (MUC13) as a candidate biomarker for ovarian cancer detection: potential to complement CA125 in detecting non-serous subtypes. *Clin. Chem. Lab. Med.* **61**, 464–472. 10.1515/cclm-2022-0491 (2023).
18. Zhang, J. et al. The role of TPS, CA125, CA15-3 and CEA in prediction of distant metastasis of breast cancer. *Clin. Chim. Acta*. **523**, 19–25. 10.1016/j.cca.2021.08.027 (2021).
19. Bhardwaj, P. V. et al. Male Breast Cancer: a Review on Diagnosis, Treatment, and Survivorship. *Curr. Oncol. Rep.* **26**, 34–45. 10.1007/s11912-023-01489-z (2024).
20. Cai, R. et al. A non-invasive preoperative prediction model for predicting axillary lymph node metastasis in breast cancer based on a machine learning approach: combining ultrasonographic parameters and breast gamma specific imaging features. *Radiat. Oncol.* **19**, 63. 10.1186/s13014-024-02453-2 (2024).
21. Esposto, G. et al. Shear-wave elastography to predict hepatocellular carcinoma after hepatitis C virus eradication: A systematic review and meta-analysis. *World J. Gastroenterol.* **30**, 1450–1460. 10.3748/wjg.v30.i10.1450 (2024).
22. Kwon, M. R. et al. Correlation of shear-wave elastography stiffness and apparent diffusion coefficient values with tumor characteristics in breast cancer. *Sci. Rep.* **14**, 7180. 10.1038/s41598-024-57832-2 (2024).
23. Asafu, A. et al. Shear Wave Elastography in Breast Cancer: Unveiling Correlations With Histopathological Grades and Subtypes. *Cureus* **16**, e63759. 10.7759/cureus.63759 (2024).
24. Qian, Q. et al. Shear-wave elastography predicts T-restaging and pathologic complete response of rectal cancer post neoadjuvant chemoradiotherapy. *Abdom. Radiol. (NY)*. **49**, 2561–2573. 10.1007/s00261-024-04361-1 (2024).
25. Liang, J. F. et al. Usefulness of Shear Wave Elastography in Determining the Tumor Extent of Basal Cell Carcinomas. *J. Ultrasound Med.* **42**, 971–976. 10.1002/jum.16104 (2023).

Figures

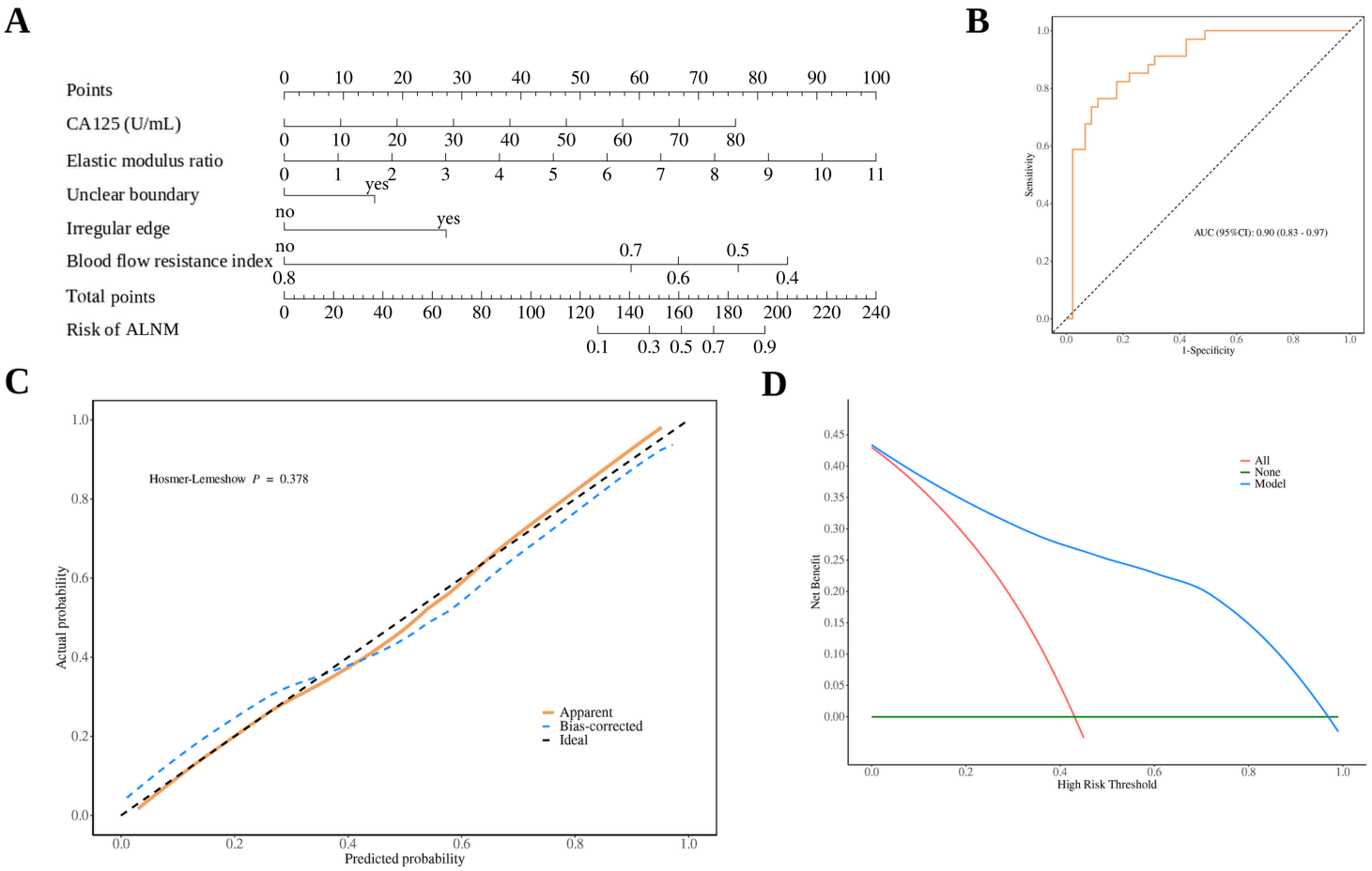


Figure 1

Construction and evaluation of a nomogram prediction model in training set. (A) Predictive model for risk of axillary lymph node metastasis (ALNM) was visualized with a nomogram. (B) Result of receiver operating characteristic (ROC) curve analysis. (C) Result of calibration curve-based analysis. (D) Result of decision curve analysis (DCA).

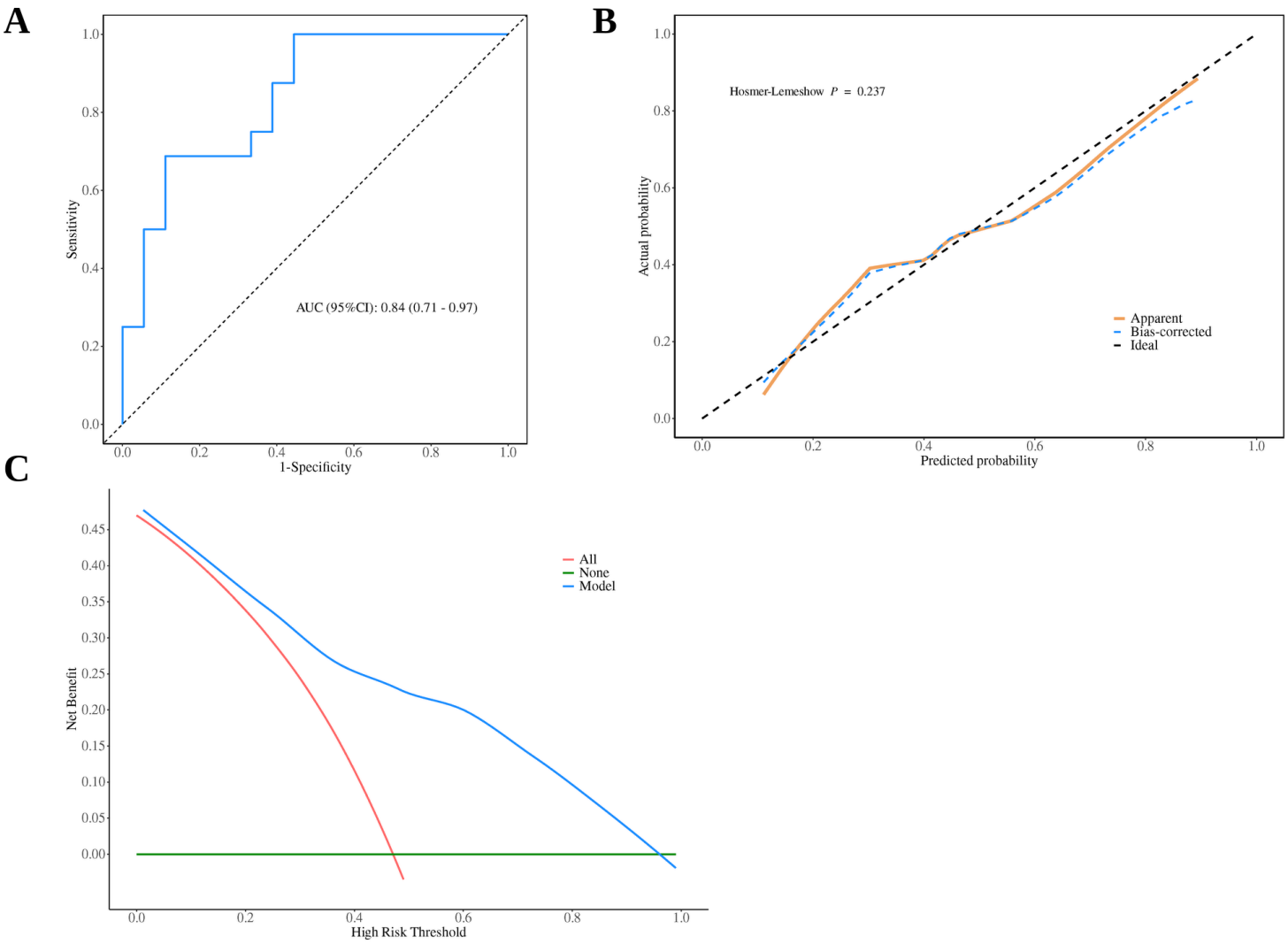


Figure 2

Validation of the clinical applicability of the nomogram prediction model in the internal validation cohort. (A) Result of receiver operating characteristic (ROC) curve analysis. (B) Result of calibration curve-based analysis. (C) Result of decision curve analysis (DCA).

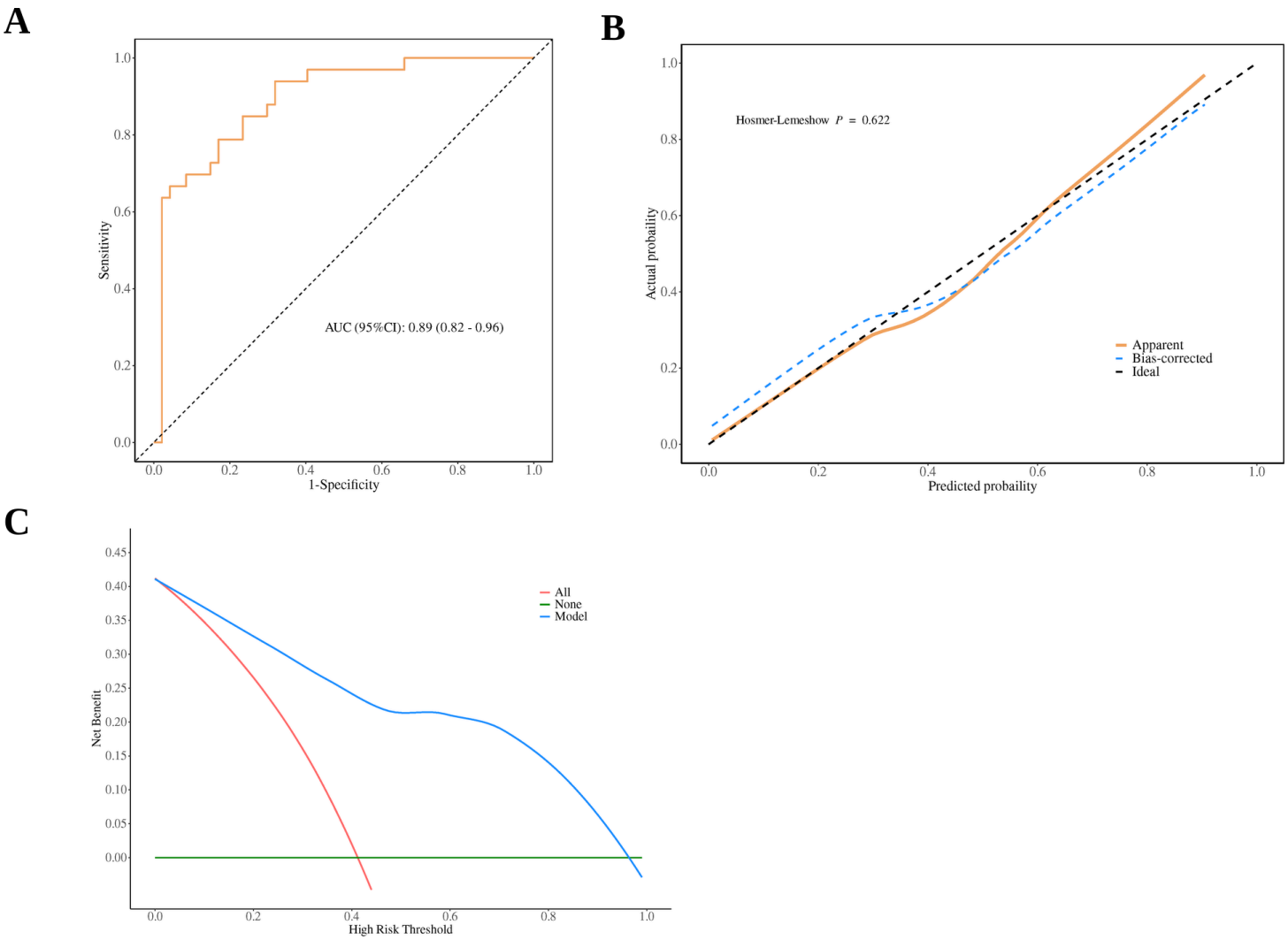


Figure 3

Validation of the clinical applicability of nomogram prediction model in the external validation data. (A) Result of receiver operating characteristic (ROC) curve analysis. (B) Result of calibration curve-based analysis. (C) Result of decision curve analysis (DCA).